The design and testing of a cooling system using mixed solid cryogen for a portable superconducting magnetic energy storage system

2010 Supercond. Sci. Technol. 23 125006

(http://iopscience.iop.org/0953-2048/23/12/125006)

Supercond. Sci. Technol. **23** (2010) 125006 (7pp) doi:10.1088/0953-2048/23/12/125006

The design and testing of a cooling system using mixed solid cryogen for a portable superconducting magnetic energy storage system

K L Kim[1], J B Song[1], J H Choi[2], S H Kim[2], D Y Koh[3], K C Seong[4], H M Chang[5] and H G Lee[1,6]

[1] Division of Materials Science and Engineering, Korea University, Seoul, Korea
[2] Department of Electrical Engineering, Gyeongsang National University and ERI, JinJu, Korea
[3] Korea Institute of Machinery and Materials, Daejeon, Korea
[4] Korea Electrotechnology Research Institute, Changwon, Korea
[5] Department of Mechanical and System Design Engineering, Hong Ik University, Seoul, Korea

E-mail: haigunlee@korea.ac.kr

Received 18 July 2010, in final form 13 October 2010
Published 29 October 2010
Online at stacks.iop.org/SUST/23/125006

Abstract
A cooling system that uses solid nitrogen (SN2) as an effective heat capacity enhancer was recently introduced to enhance the thermal stability of the HTS SMES. Since SN2 has a large enthalpy with minimal weight, it enables a portable system by increasing the recooling to recooling time period (RRTP). However, contact between the SN2 and HTS SMES magnet can be broken by repeated thermal disturbances (thermal 'dry-out' phenomena). Therefore, it is essential to improve thermal contact to allow full use of the heat capacity of SN2. This study evaluated the effect of using a mixture containing SN2 and a small amount of a liquid cryogen as a cooling system in the HTS SMES system. The performance of the cooling system was evaluated using the mixed cryogen and compared with that of SN2 alone. In addition, the role of liquid neon (Ne) as a heat exchanger between SN2 and the HTS SMES magnet is discussed.

(Some figures in this article are in colour only in the electronic version)

1. Introduction

With the increasing demand for electricity since the early 1980s, the possibility of sudden electric power interruptions has also increased. These can cause serious damage to electrical equipment or manufacturing facilities. Various types of power quality compensating devices, such as storage batteries and electrolytic capacitors, have been installed in power systems to prevent this problem. However, such devices lead to serious environmental pollution and occupy a large space. The SMES is an alternative solution, and many SMES systems have been developed and evaluated. In particular, SMES systems fabricated using BSCCO-2223 tapes have the advantage of rapid charging and recharging and can be used as an uninterruptible power supply (UPS) [1–5].

Generally, the cooling system for a SMES system uses conduction cooling through a cryocooler or a liquid cryogen to cool the HTS magnet [6, 7]. While conduction cooling is a convenient way to operate, it cannot maintain the operating temperature of the HTS magnet and the cryocooler needs to be operated continuously. In the case of a cooling system using a liquid cryogen, such as liquid He (LHe) or liquid Ne (LNe), the operating temperature is fixed to its vaporization temperature. Moreover, the system experiences an abrupt increase in pressure due to Joule heating when the HTS magnet is quenched.

[6] Author to whom any correspondence should be addressed.

According to recent studies, a solid cryogen possessing a large heat capacity can enable HTS application systems to utilize the ability of the HTS magnet to maintain a constant field over a wide operating range [8–13]. Having a large enthalpy with minimal weight, the solid cryogen makes possible a compact and portable HTS SMES system with increased recooling to recooling time period (RRTP) [14]. However, a cooling system using SN2 has potential thermal contact problems from repeated thermal disturbances, such as local heating or over-current (thermal dry-out phenomena). To enhance the thermal contact between the solid cryogen and the HTS SMES magnet, this study proposes a mixed cryogen for a HTS SMES using a mixture containing a solid cryogen (i.e., SN2) and small amounts of a liquid cryogen (i.e., LNe). A cooling system that uses a mixed cryogen for an HTS SMES system was designed and fabricated. The cooling performance of the mixed cryogen was compared with that of SN2 alone. The role of the LNe as an effective heat exchanger was also evaluated through quench tests of the HTS SMES system.

2. Calculation of the heat inputs into the system

In order to create an optimal design of the cooling system, it is essential to obtain the precise value of the total heat input into the SMES system. The total heat input (Q_{total}) can be calculated by summing the heat input by conduction (Q_{cond}), radiation (Q_{rad}) and convection (Q_{conv}). Q_{cond} can be determined using the following equation [15, 16]:

$$Q_{\text{cond}} = \frac{A_{\text{cond}}}{x}\int_{T_1}^{T_2} k(T)\,\mathrm{d}T \tag{1}$$

where A_{cond} and x are total cross-section area and entire length of the conductors including four support rods, four current leads and LNe and LN2 inlet tubes, etc in this study. T_1 and T_2 are the temperatures of both ends of the conductor ($T_2 > T_1$). k is the thermal conductivity of the conductor as a function of temperature (T). The calculated heat input by conduction due to the current leads was almost 76% of the total Q_{cond} value (17.56 W).

Generally, the radiation heat input, Q_{rad}, is determined using the Stefan–Boltzmann equation:

$$Q_{\text{rad}} = e_r \sigma_{\text{SB}} T^4 S \tag{2}$$

where e_r is the total emissivity at temperature T, σ_{SB} is the Stefan–Boltzmann constant (5.67×10^{-8} W m^{-2} K^{-4}) and S is the total area of the surface. The cryostat used in the study has a 'parallel-plate' configuration, so that equation (2) can be modified as follows:

$$q_{\text{rad}} = [e_{\text{r}}]_{\text{cw}} \sigma_{\text{SB}} ({T_{\text{wm\_in}}}^4 - {T_{\text{cl\_in}}}^4) \tag{3}$$

where $T_{\text{wm\_in}}$ and $T_{\text{cl\_in}}$ are the temperatures of each surface at the warm (77 K at the radiation shield) and cold temperature (20 K at the SN2 vessel), respectively. For the configuration of parallel plates with emissivities of $[e_r]_{\text{cl}}$ and $[e_r]_{\text{wm}}$ at T_{cl} and T_{wm}, respectively, the effective total emissivity, $[e_r]_{\text{cw}}$, can be given by the following [16]:

$$[e_r]_{\text{cw}} = \frac{[e_r]_{\text{cl}}[e_r]_{\text{wm}}}{[e_r]_{\text{cl}} + [e_r]_{\text{wm}} - [e_r]_{\text{cl}}[e_r]_{\text{wm}}}. \tag{4}$$

Table 1. Parameters used to calculate the radiative heat flux.

Parameters	Specifications
Stefan–Boltzmann constant (σ_{SB}) (W m^{-2} K^{-4})	5.67×10^{-8}
Total number of superinsulation layers (N) (turns)	10
Radiative heat flux to the SN2 vessel (q_{rad}) (W m^{-2})	0.0164
Total area of the surface of SN2 vessel (m^2)	1.5798

Table 2. Values of the heat inputs.

Heat input	Values
Conduction heat input (Q_{cond}) (W)	17.56
Radiation heat input (Q_{rad}) (W)	0.022
Total heat input (Q_{total}) (W)	17.582

Table 3. Specifications of the BSCCO-2223 DP coil for the HTS SMES magnet.

Parameters	Specifications
Inner diameter (mm)	500
Outer diameter (mm)	697
I_{c} (A) (@ 77 K)	120
Inductance (mH)	~70
Total length of the conductor (m)	490

In general, several layers of superinsulation were wound around the radiation shield. Therefore, the presence of superinsulation layers modifies equation (3) to

$$q_{\text{rad}} = \frac{[e_r]_{\text{cw}}}{N+1}\sigma_{\text{SB}}({T_{\text{wm\_out}}}^4 - {T_{\text{cl\_out}}}^4) \tag{5}$$

where $T_{\text{wm\_out}}$ and $T_{\text{cl\_out}}$ are 77 K and 20 K, respectively, and N is the total number of the superinsulation layers (e.g., $N = 10$ in this study). Table 1 lists the parameters used to calculate the radiative heat flux.

The convective heat transfer by the residual gas (Q_{conv}) can also be given by

$$Q_{\text{conv}} = hA_{\text{conv}}(T_{\text{wm}} - T_{\text{cl}}) \tag{6}$$

where h is the convective heat coefficient and A_{conv} is the surface area of heat transfer, respectively. Q_{conv} can be neglected because the SN2 vessel is completely vacuum-sealed (pressure $\approx 10^{-7}$ Torr) and there is no additional gas input into the SN2 vessel. Table 2 summarizes the calculated heat input of the cooling system used in this study.

3. Experimental setup

3.1. BSCCO-2223 DP coil

Figure 1 shows a photograph of the BSCCO-2223 double pancake (DP) coil for the HTS SMES magnet used in this study. The minimum inner and outer diameters were 500 mm and 697 mm, respectively. The minimum gap between the top and bottom pancake was 1 mm. Before the quench tests, the critical currents (I_{c}) of the DP coil were measured using the criterion of 1 μV cm^{-1}. The self-field I_{c} value of the DP coil measured in a bath of LN2 (77 K) was 120 A. Table 3 lists the specifications of the DP coil.

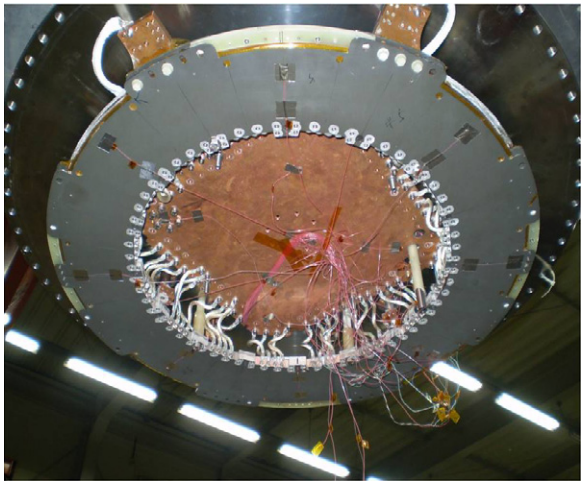

Figure 1. Photograph of the BSCCO-2223 DP coil.

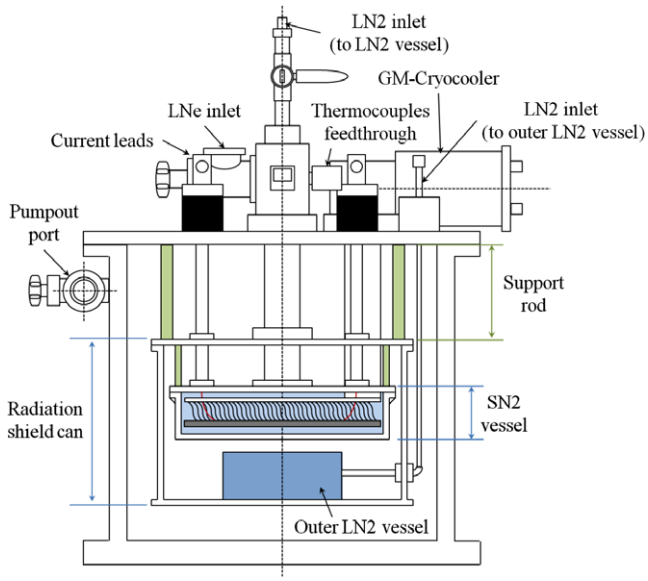

Figure 3. Schematic diagram of a cross-section of the cooling system.

3.2. Cooling system using a solid nitrogen (SN2)

Figure 2 shows a schematic diagram of the experimental setup. The SN2 cooling system was composed of a SN2 vessel, a radiation shield can, a feedthrough for the thermocouples and voltages tapes, four current leads, one vacuum pump-out port, one pressure gauge and a two-stage GM-cryocooler (Daikin U110MDW). The first and second stages of the cryocooler have cooling capacities of 35 W and 0.8 W at 41 K and 4.2 K, respectively. Figure 3 shows a schematic diagram of a cross-section of the SN2 cooling system. The vacuum pump was connected to the pump-out port and a pressure of 10^{-7} Torr inside the cryostat was maintained to minimize radiation and convection heat input into the SN2 vessel. In addition, an outer LN2 vessel was installed at the bottom of the radiation shield can to maintain the temperature of the radiation shield at 77 K.

Figure 4 shows a schematic drawing of the SN2 vessel, made of stainless steel, for SN2 (80 ℓ) and a DP coil. The coldhead of the cryocooler was connected thermally to the DP coil using a bunch of oxygen-free high conductivity copper (OFHC) wires insulated with Kapton tape. As shown in figure 4(b), a heater in the form of a Fe–Cr strip was installed at the bottom DP coil to generate a local hot spot during the quench tests. The dimensions and resistance of the Fe–Cr strip were 4 mm × 10 mm and 5 Ω, respectively. A total of 8 V taps were attached to the right side of the Fe–Cr heater at intervals of 5 cm. To obtain the temperature profiles inside the SN2 vessel, 28 E-type thermocouples were installed in the

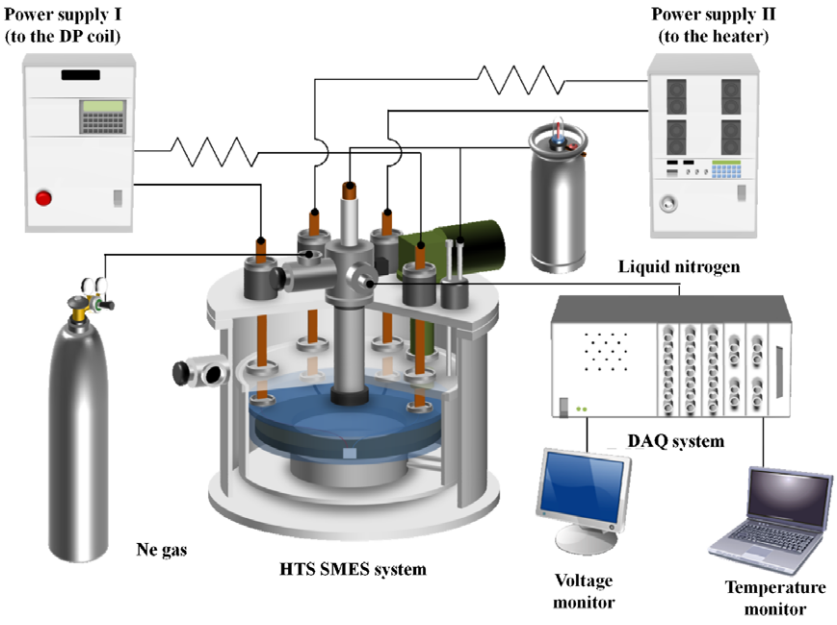

Figure 2. Schematic diagram of the experimental setup.

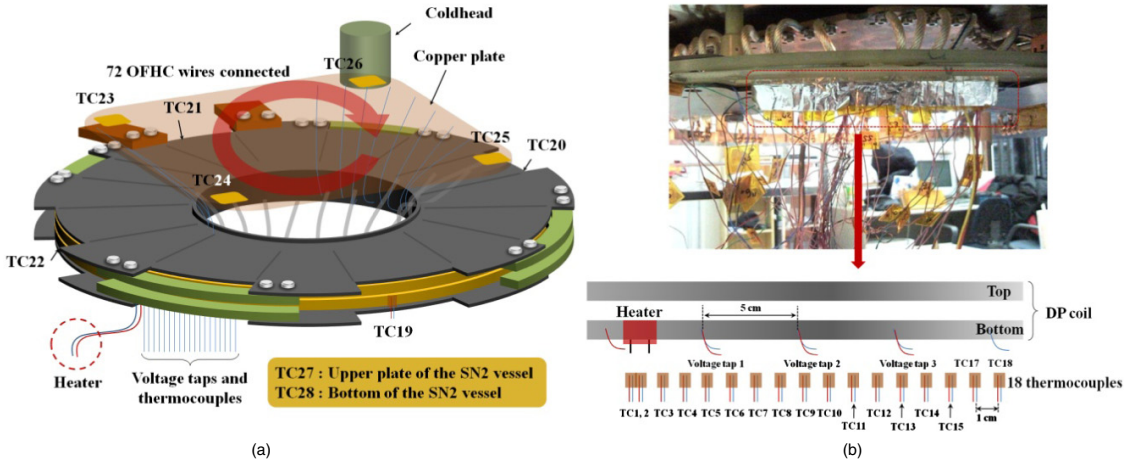

Figure 4. (a) Schematic drawing of the BSCCO-2223 DP coil for SMES and (b) voltage taps and thermocouples attached on the bottom coil.

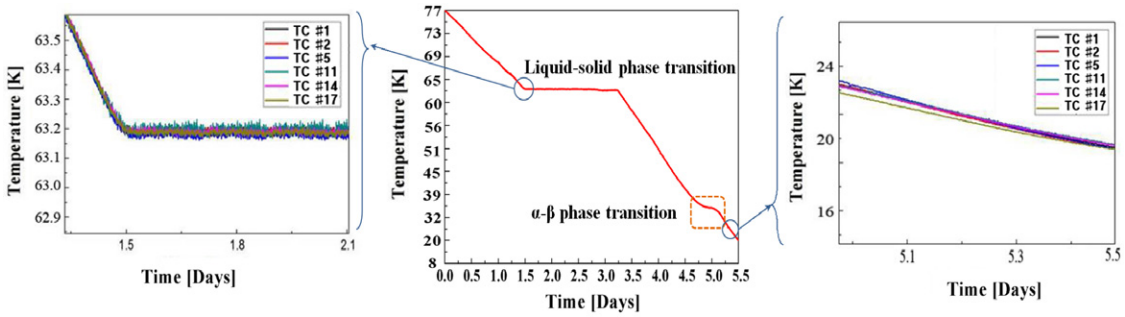

Figure 5. Cooling profile of N_2 from 77 to 20 K as a function of time.

following positions: (1) on the heater (TC1, TC2), (2) on the right side (TC3–TC18:1 cm interval) of the heater, (3) along the side of the DP coil (TC19–TC22), and (4) on the bottom of the copper plate with an attached coldhead (TC23–TC26). TC27 and TC28 were located on the upper plate and bottom of the SN2 vessel, respectively. The temperature was monitored continuously and recorded using a data acquisition (DAQ) system (NI PXI-4071).

The SN2 vessel was sealed completely with an aluminum gasket and filled with LN2. The LN2 was then slowly solidified and cooled at constant cooling rate of 7.40 mK s^{-1} to an operating temperature of 20 K using a GM-cryocooler.

3.3. Cooling system using a mixed cryogen

In the case of a cooling system using the mixed cryogen, the setup was similar to that in the SN2 cooling system. The only difference between the two systems was the cryogen. The mixed cryogen was produced by a mixture of Ne gas and SN2. Ne gas was injected directly into the SN2 vessel at 27 K after the LN2 had solidified. The cryogen was then liquefied using a GM-cryocooler. The flow rate of the Ne gas (100–200 cc min^{-1}) was maintained using a gas flow controller. The total amount of liquid Ne can be estimated by measuring the volume of Ne gas evaporated during the warm-up period using the volume ratio of Ne gas to liquid Ne (i.e. 1436).

3.4. Quench tests

Quench tests were carried out using the following process: (1) an operating current (I_{op}) was applied to the DP coil, (2) various currents were applied to the heater for 40 and 60 s to generate local hot spots, and (3) the I_{op} was maintained for a few seconds after the heater was stopped. The quench tests were carried out at sufficient time intervals (approximately 1 h) to allow the temperature of the DP coil to return to its initial temperature of 20 K. The temperature and voltage signals were monitored and recorded using the DAQ system (NI SCXI-1305) during the tests.

4. Results and discussion

4.1. Cooling performance of the SN2 cooling system

Figure 5 shows the temperature traces obtained while cooling the SN2 vessel from 77 to 20 K. The liquid–solid transition and α–β phase transition of N_2 were observed at 63.15 K and 36.5 K, respectively. The temperature reached 20 K after 5.5 days. In addition, the temperatures measured using all thermocouples were within ∼1 K. Figure 6 shows the warm-up

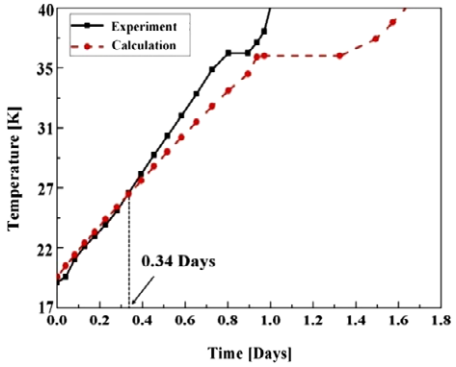

Figure 6. Warm-up performance of the SN2 as a function of time.

performance of SN2 as a function of time when the cryocooler was idle.

From the results in figure 6, the total heat input into the SN2 vessel can be calculated using the following equation [17, 18]:

$$Q_{\text{total}} = \frac{V \times \Delta H}{\Delta t} \tag{7}$$

where V is the volume of SN2 (80 ℓ), Δt is the duration (85 897 s) of the temperature variation from the initial temperature ($T_{\text{i}} = 20$ K) to the final temperature ($T_{\text{f}} = 40$ K). ΔH is the total enthalpy change of SN2 as follows:

$$\Delta H = \int_{T_{\text{i}}}^{T_{\text{f}}} C_p(T)\,\mathrm{d}t \tag{8}$$

where C_p is the specific heat of SN2. The ΔH value determined using equation (8) was 28.54 J cm^{-3}. The measured Q_{total} value was 26.58 W, which is 49% higher than that obtained from theory (17.59 W). This discrepancy suggests that extra heat input into the SN2 vessel was generated during warm-up. The extra heat was due to the increase in temperature of the radiation shield because the amount of LN2 supplied to the outer LN2 vessel kept decreasing during the warm-up period. Therefore, until 0.34 days, the two temperature profiles obtained from the experiment and calculation (theory) were similar. However, the discrepancy between them became larger after 0.34 days (see figure 6).

4.2. Quench tests of the DP coil in the cooling system using the SN2

Figure 7 shows $V(t)$ traces of the DP coil during the quench tests at 20 K and $I_{\text{op}} = 72$ A (60% of I_{c} (at 77 K)), 84 A (70%) and 96 A (80%) in the SN2 cooling system. The current applied to the heater was 9 A for 60 s, corresponding to a heater energy (E_{heater}) of 972 J. As shown in figure 7(a), there was no increase in magnet voltage during the quench test, which suggests that quenching did not occur at $I_{\text{op}} = 72$ A. However, at $I_{\text{op}} = 96$ A, the voltage increased abruptly and reached the peak voltage (V_{peak}) of 1.3 V.

To examine the change in thermal contact between SN2 and the DP coil, quench tests at $E_{\text{heater}} = 648$ J were carried out at sufficient time intervals (approximately 1 h), so that the temperature of the DP coil returned to the initial temperature of 20 K. The reason for selecting the lower E_{heater} (i.e., 648 J) than that (972 J) in previous tests was to prevent damage to the DP coil during the tests. As shown in figure 8, quenching occurred, even at $I_{\text{op}} = 72$ A, but not in the case of the test at $E_{\text{heater}} = 972$ J. Moreover, the V_{peak} values at $I_{\text{op}} = 84$ A and 96 A were 2 and 3.8 V, respectively, which are larger than those (0.13 and 1.3 V) obtained at $E_{\text{heater}} = 972$ J. These test results using SN2 alone confirmed that thermal contact between the SN2 and DP coil become separated by Joule heating during the quench tests, resulting in a 'thermal dry-out' problem in the cooling system.

4.3. Quench tests of the DP coil in the cooling system using the mixed cryogen

Another set of quench tests were carried out at 20 K in the cooling system using the mixed cryogen to evaluate the role of the liquid cryogen as an effective heat exchanger. When the temperature of the SN2 was set to 27 K, Ne gas was injected into the SN2 vessel and liquefied using a GM-cryocooler. Finally, the mixed cryogen consisted of SN2 (80 ℓ) and a small amount of liquid Ne (0.0125 ℓ), which is 0.016% of the total volume of SN2. The quench tests were performed at the same I_{op} values (i.e., 72, 84 and 96 A) as those used in the SN2 cooling system.

Figures 9 and 10 show $V(t)$ traces of the DP coil measured at 20 K with $E_{\text{heater}} = 648$ J and 1254 J, respectively. As shown in figure 9, unlike the SN2 cooling system, no quench signals were detected in any of the quench tests at $E_{\text{heater}} = 648$ J

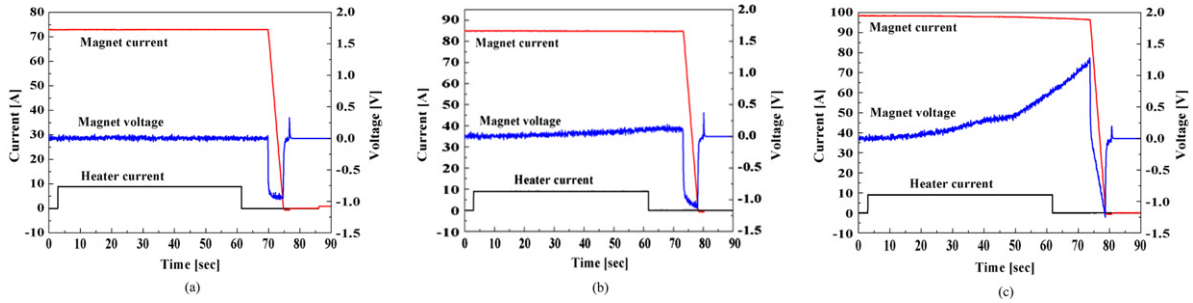

Figure 7. Voltage traces of the DP coil measured at 20 K at $E_{\text{heater}} = 972$ J, $I_{\text{op}} = 72$ A (a), 84 A (b) and 96 A (c) in the cooling system using a SN2.

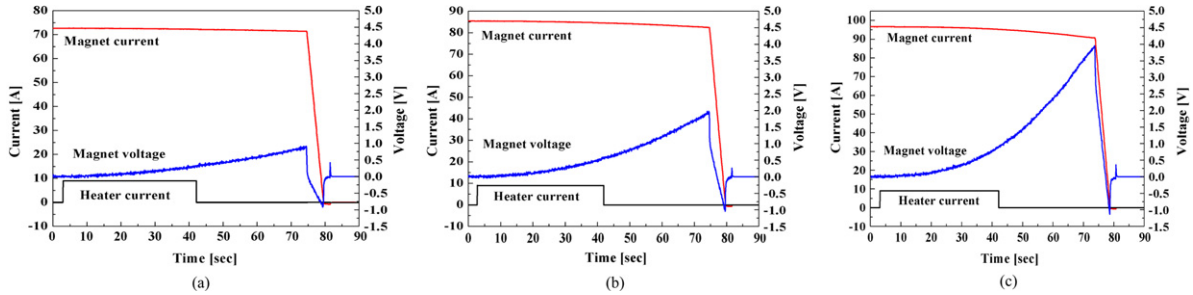

Figure 8. Voltage traces of the DP coil measured at 20 K at $E_{\text{heater}} = 648$ J, $I_{\text{op}} = 72$ A (a), 84 A (b) and 96 A (c) in the cooling system using SN2.

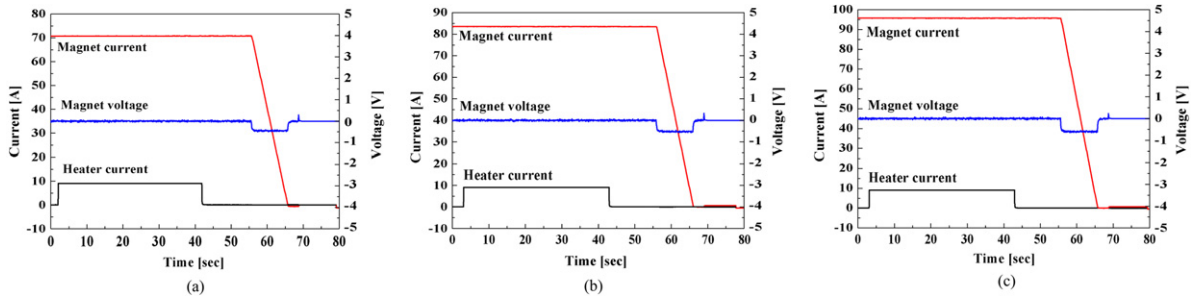

Figure 9. Voltage traces of the DP coil measured at 20 K at $E_{\text{heater}} = 648$ J, $I_{\text{op}} = 72$ A (a), 84 A (b) and 96 A (c) in the cooling system using a mixed cryogen.

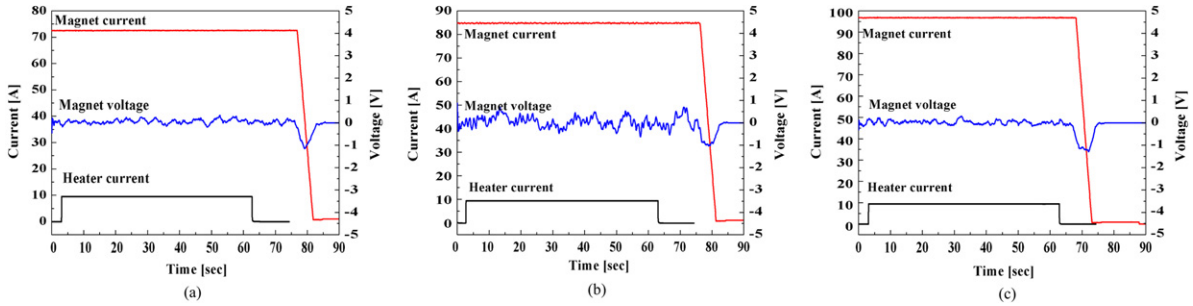

Figure 10. Voltage traces of the DP coil measured at 20 K at $E_{\text{heater}} = 1254$ J, $I_{\text{op}} = 72$ A (a), 84 A (b) and 96 A (c) in the cooling system using a mixed cryogen.

in the cooling system using the mixed cryogen. In addition, $V(t)$ traces at even higher E_{heater} (i.e., 1254 J) showed that quenching did not occur (see figure 10).

The effect of E_{heater} on the thermal stability of the DP coil in a mixed cryogen cooling system was examined by performing quench tests at various E_{heater} (1392, 1560, 1792 and 1972 J), which were greater than those in the previous tests (i.e., 972, 648 and 1254 J). Figure 11 shows the $V(t)$ traces of the DP coil measured at 20 K at $I_{\text{op}} = 96$ A in the cooling system using a mixed cryogen. As expected, the V_{peak} value increased with increasing E_{heater}. The DP coil was quenched after the quench test at $E_{\text{heater}} = 1560$ J but recovered immediately during the test. This did not occur in the case of the SN2 cooling system (i.e., $V(t)$ traces increased continuously, as shown in figures 7 and 8).

Overall, this study clearly demonstrates that the thermal stability of the DP coil for a HTS SMES magnet subjected to local hot spots was enhanced significantly by impregnating SN2 with a small amount of liquid Ne.

5. Conclusion

This study examined the thermal stability of a DP coil in both cooling systems using SN2 alone and a mixture of SN2 and small amounts of liquid Ne. The quench tests confirmed that the DP coil was more thermally stable in the cooling system using the mixed cryogen than SN2 alone, where thermal contact between SN2 and the DP coil become broken by Joule heating during the quench tests, resulting in 'thermal dry-out'. Moreover, the DP coil recovered immediately in the mixed cryogen cooling system, even when quenching occurred during the quench test, but not when SN2 alone was employed. These results suggest that liquid Ne plays the role of an effective heat exchanger that enhances the heat transfer between the DP coil

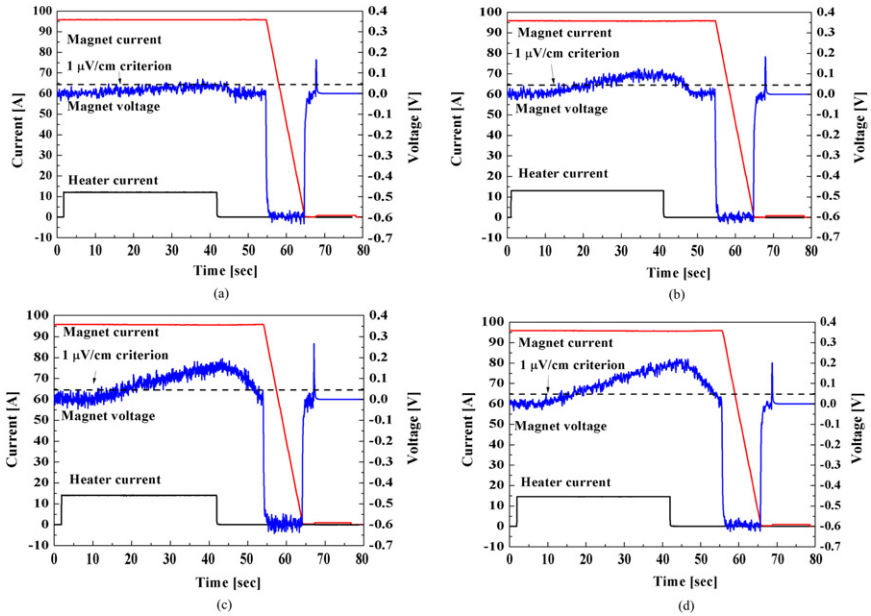

Figure 11. Voltage traces of the DP coil measured at 20 K at $I_{op} = 96$ A, $E_{heater} = 1392$ J (a), 1560 A (b), 1792 J (c) and 1972 J (d) in the cooling system using a mixed cryogen.

and SN2. Further studies on cooling systems using a mixed cryogen with respect to the total amount of mixed liquid Ne will be needed to determine its effect on the thermal/electrical stability of the DP coils for the HTS SMES system in a SN2 cooling system.

Acknowledgment

This study was supported by the Electric Power Industry Technology Evaluation and Planning.

References

[1] Park M J, Kwak S Y, Kim W S, Lee S W, Lee J K, Choi K D, Jung H K, Seong K C and Hahn S Y 2007 Analysis of magnetic field distribution and AC losses of a 600 kJ SMES *Cryogenics* **47** 391–6

[2] Kim H J, Seong K C, Cho J W, Bae J H, Sim K D, Ryu K W, Seok B Y and Kim S H 2006 Development of a 3 MJ/750 kVA SMES system *Cryogenics* **46** 367–72

[3] Seong K C, Kim H J, Kim S H, Park S J, Woo M H and Hahn S Y 2007 Research of a 600 kJ HTS-SMES system *Physica* C **463–465** 1240–6

[4] Kim S, Sohn M H, Sim K and Seong K C 2007 Test result of the model coil for the conduction cooled HTS SMES *Physica* C **463-465** 1257–61

[5] Seong K C, Kim H J, Kim S W, Cho J W, Kwon Y K, Ryu K S, Yu I K and Hahn S Y 2002 Current status of SMES in Korea *Cryogenics* **42** 351–5

[6] Friedman A, Shaked N, Perel E, Sinvani M, Wolfus Y and Yeshurun Y 1999 Superconducting magnetic energy storage device operating at liquid nitrogen temperatures *Cryogenics* **39** 53–8

[7] Ishiyama A, Akita S, Kasahara H and Sakaguchi H 2001 Research and development of HTS-SMES system *Physica* C **357–360** 1311–4

[8] Yao W, Bascuñán J, Kim W, Hahn S, Lee H and Iwasa Y 2008 A solid nitrogen cooled MgB_2 'demonstration' coil for MRI applications *IEEE Trans. Appl. Supercond.* **18** 912–5

[9] Bascuñán J, Lee H G, Bobrov E S, Hahn S Y, Iwasa Y, Tomsic M and Rindfleisch M 2006 A 0.6 T/650 mm RT bore solid nitrogen cooled MgB_2 demonstration coil for MRI-a status report *IEEE Trans. Appl. Supercond.* **16** 1427–30

[10] Nakamura T, Muta I, Okude K, Fujio A and Hoshino T 2002 Solidification of nitrogen refrigerant and its effect on thermal stability of HTSC tape *Physica* C **372–6** 1434–7

[11] Haid B J, Lee H G, Iwasa Y, Oh S S, Ha H, Kwon Y K and Ryu K S 2001 Stand-alone solid nitrogen cooled permanent high-temperature superconducting magnet system *IEEE Trans. Appl. Supercond.* **11** 2244–7

[12] Song J B, Kim K L, Kim K J, Lee J H, Kim H M, Kim W S, Yim S W, Kim H-R, Hyun O B and Lee H G 2008 The design, fabrication and testing of a cooling system using solid nitrogen for resistive high-T_c superconducting fault current limiter *Supercond. Sci. Technol.* **21** 115023

[13] Iwasa Y, Bascuñán J, Hahn S and Yao W 2009 High-temperature superconductors for NMR/MRI magnets: opportunities and challenges *Supercond. Cryog.* **11** 1–7

[14] Iwasa Y, Wheatley R, Bascuñán J, Haid B and Lee H 2003 A solid-nitrogen cooled Nb_3Sn NMR magnet operating in the range 8–10 K *IEEE Trans. Appl. Supercond.* **13** 1636–9

[15] Lee H G, Kim H M, Lee B W, Oh I S, Kim H-R, Hyun O B, Sim J, Chang H M, Bascuñán J and Iwasa Y 2007 Conduction-cooled brass current leads for a resistive superconducting fault current limeter (SFCL) system *IEEE Trans. Appl. Supercond.* **17** 2248–51

[16] Iwasa Y 2009 *Case Studies in Superconducting Magnets-Design and Operational Issues* 2nd edn (New York: Springer)

[17] Haid B J, Lee H G, Iwasa Y, Oh S S, Kwon Y K and Ryu K S 2002 A permanent high-temperature superconducting magnet operated in thermal communication with a mass of solid nitrogen *Cryogenics* **42** 229–44

[18] Haid B J, Lee H G, Iwasa Y, Oh S S, Ha H, Kwon Y K and Ryu K S 2002 Design analysis of a nitrogen cooled permanent high-temperature superconducting magnet system *Cryogenics* **42** 617–34